

Spectralmatch: relative radiometric normalization toolkit for raster mosaics and time series

Kanoa Lindiwe  ¹, Joseph Emile Honour Percival  ¹, and Ryan Perroy  ^{1,2}

¹ Spatial Data Analysis & Visualization Research Lab, University of Hawaii at Hilo, United States 
Dept of Geography & Environmental Science, University of Hawaii at Hilo, United States 

DOI: [10.21105/joss.08974](https://doi.org/10.21105/joss.08974)

Software

- [Review](#) 
- [Repository](#) 
- [Archive](#) 

Editor: [Ethan White](#)  

Reviewers:

- [@Digggeo](#)
- [@ethanwhite](#)

Submitted: 07 July 2025

Published: 23 January 2026

License

Authors of papers retain copyright and release the work under a Creative Commons Attribution 4.0 International License ([CC BY 4.0](#)).

Summary

Spectralmatch provides algorithms to perform relative radiometric normalization (RRN) to enhance spectral consistency across raster mosaics and time series. It is built for geoscientific use, with a sensor- and unit-agnostic design, optimized for automation and efficiency on arbitrarily many images and bands, and works well with Very High Resolution Imagery (VHRI) as it does not require pixel co-registration. Its current matching algorithms are inspired by Yu et al. (2017), which include global regression and local block adjustment which minimize inter-image variability without relying on ancillary data. The impact of these functions on spectral consistency is illustrated in Figure 1. The software supports cloud and vegetation masking, pseudo invariant feature (PIF) based exclusion, seamline network generation, raster merging, and plotting statistics. The toolkit is available as an open-source Python library, command line interface, and QGIS plugin.

Statement of Need

Remote sensing relies on mosaics to broaden spatial coverage, and on time series to extend temporal coverage. However, both are affected by inter-image spectral variability, caused by differences in the atmosphere, illumination, surface condition, acquisition geometry, and other complications (Theiler et al., 2019). These factors introduce inconsistencies, reduce analytical accuracy, and complicate the detection of actual environmental changes. To address these issues, researchers have explored two main correction approaches in the literature: absolute radiometric correction and RRN, or a combination of both (Hu et al., 2011). The absolute approach corrects for the aforementioned inaccuracies with algorithms involving atmospheric correction and bidirectional reflectance distribution functions (Shen et al., 2025), and gains accuracy from in-situ measurements, which may not exist or be difficult to obtain for specific images (Canty et al., 2004). Conversely, the relative approach applies algorithms to minimize apparent spectral differences between images, matching them for consistent analysis, rather than determining true spectral values or relying on ancillary data.

Researchers have examined various algorithms for performing RRN (Vorovencii & M., 2014), with model selection and the identification of PIFs recognized as among the most critical and challenging aspects (Hessel et al., 2020). Most researched RRN methods are not integrated into software packages, which leaves subsequent researchers either spending significant time implementing their own versions of the algorithms or relying on the limited available tools. There are commercial software programs that implement RRN which include ArcGIS Pro (dodging, global fit, histogram, and standard deviation), ENVI (histogram matching), ERDAS IMAGINE Mosaic Pro (illumination equalizing, dodging, color balancing, and histogram matching) and others. In addition, open source solutions include QGIS (histogram matching and Iteratively Reweighted Multivariate Alteration Detection (IR-MAD)), MATLAB scripts (pixel similarity

grouping by Moghimi et al. (2024)), Python scripts (multi-sensor normalization by Hessel et al. (2020)) and the R ‘landsat’ library (histogram matching, pixel-wise linear regression, K-T ratio, and urban materials ratio) by Goslee (2011). While existing solutions cover many use cases, there is not an open source, scalable library to match non-coregistered VHRI using the mean-standard deviation method which this library specifically addresses. In addition, this library provides an extensible structure to add new RRN methods to meet researchers’ varying needs and dataset requirements.

Implemented RRN Methods

The current matching algorithm uses a two-step approach involving global regression and local block adjustment following the methods of Yu et al. (2017). The approach is suitable to match imagery from the same sensor or from multiple sensors with comparable wavelengths and resolution—for example, between satellites (Sentinel-PlanetScope) or between drones (Zenmuse P1-Mavic 3 Multispectral). The global regression algorithm adjusts brightness and contrast across overlapping images to reduce spectral differences. It first detects overlapping image pairs and computes per-band statistics (mean and standard deviation) within those regions. Using these statistics, a least-squares regression system is constructed to solve for per-image, per-band scale and offset parameters that minimize radiometric differences in overlapping areas. This approach aims to minimize brightness and contrast differences across images while preserving global consistency and aligning the spectral profiles of images to a central tendency, specific image, or set of images via custom-weighted mean and standard deviation constraints.

The local block adjustment algorithm applies block-wise radiometric correction to individual satellite images based on local differences from a reference mosaic. The method divides the combined extent of all input images into spatial blocks and calculates local mean statistics for each block. Each image is then locally adjusted using interpolated adaptive gamma normalization to align with the global reference mosaic. This allows radiometric consistency across spatially heterogeneous scenes on a block scale. Both global and local algorithms support nodata-aware processing for images of irregular shapes and internal gaps and vector PIF masking applied at the matching solution stage. For large datasets, the library supports cloud optimized geotiff outputs, saving and loading of intermediate steps, and efficient windowing and parallelization. For example, on a computer with 16GB of memory and 10 M1 cores, multiprocessing increased processing speed by up to 43%, with larger images showing larger increases.

Various helper functions support the creation of cloud masks, non-vegetation PIFs, generating seamline networks, merging images, and basic figures. Cloud masking utilities enable the generation of binary masks using *OmniCloudMask* by Wright et al. (2025), followed by post-processing and vectorization. Vegetation masking utilities use NDVI-based thresholds, followed by post-processing and vectorization. The created masks can be used to mask input images or withhold pixels from analysis. Seamline generation utilities use Voronoi-based centerlines, following the methodology of Yuan et al. (2023). Statistical utilities can generate basic figures comparing image spectral profiles before and after matching to evaluate radiometric changes. Raster merging utilities combine the final images into a seamless mosaic.

Figures

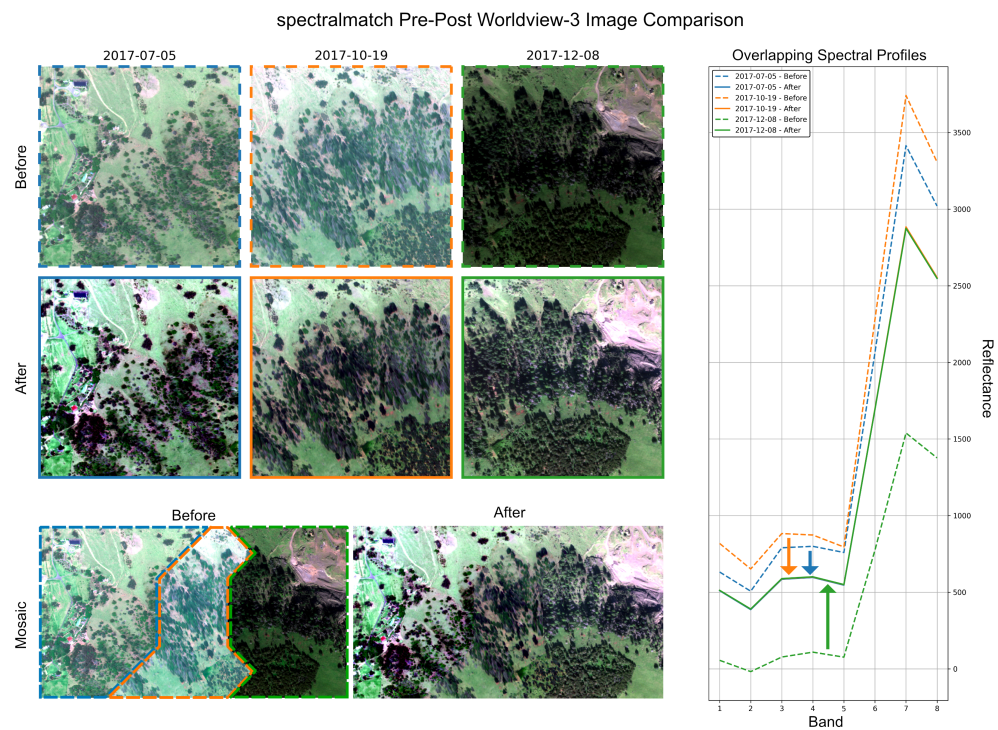


Figure 1: Comparison of three WorldView-3 images from Pu'u Wa'awa'a, Hawai'i before and after processing with global regression and local block adjustment using spectralmatch. The top left shows images before processing, the middle left shows images after processing, the bottom left shows images mosaicked before and after processing, and lastly, the right shows the averaged spectral profiles from the overlapping area of all images.

Acknowledgements

This work was primarily funded by the National Science Foundation EPSCoR grant 2149133, Change Hawai'i: Harnessing the Data Revolution for Island Resilience. The University of Hawaii at Hilo Spatial Data Analysis and Visualization Lab (SDAV) provided computational and laboratory resources.

References

- Canty, M. J., Nielsen, A. A., & Schmidt, M. (2004). Automatic radiometric normalization of multitemporal satellite imagery. *Remote Sensing of Environment*, 91(3), 441–451. <https://doi.org/10.1016/j.rse.2003.10.024>
- Goslee, S. C. (2011). Analyzing remote sensing data in R: The landsat package. *Journal of Statistical Software*, 43(4), 1–25. <https://doi.org/10.18637/jss.v043.i04>
- Hessel, C., Grompone von Gioi, R., Morel, J. M., Facciolo, G., Arias, P., & Franchis, C. de. (2020). Relative radiometric normalization using several automatically chosen reference images for multi-sensor, multi-temporal series. *ISPRS Annals of the Photogrammetry, Remote Sensing and Spatial Information Sciences*, V-2–2020, 845–852. <https://doi.org/10.5194/isprs-annals-V-2-2020-845-2020>

- Hu, Y., Liu, L., Liu, L., & Jiao, Q. (2011). Comparison of absolute and relative radiometric normalization use landsat time series images. *MIPPR 2011: Remote Sensing Image Processing, Geographic Information Systems, and Other Applications*, 8006, 283–290. <https://doi.org/10.1117/12.902076>
- Moghimi, A., Sadeghi, V., Mohsenifar, A., Celik, T., & Mohammadzadeh, A. (2024). LIRRN: Location-independent relative radiometric normalization of bitemporal remote-sensing images. *Sensors*, 24(7). <https://doi.org/10.3390/s24072272>
- Shen, A., Shao, J., Qi, X., Zhu, Z., Dai, Y., & Zeng, Q. (2025). BRDF correction in landsat directional reflectance data by combining optimal BRDF archetype with spectral characteristics. *IEEE Journal of Selected Topics in Applied Earth Observations and Remote Sensing*, 18, 17592–17609. <https://doi.org/10.1109/JSTARS.2025.3586463>
- Theiler, J., Ziemann, A., Matteoli, S., & Diani, M. (2019). Spectral variability of remotely sensed target materials: Causes, models, and strategies for mitigation and robust exploitation. *IEEE Geoscience and Remote Sensing Magazine*, 7(2), 8–30. <https://doi.org/10.1109/MGRS.2019.2890997>
- Vorovencii, I., & M., D. M. (2014). Relative radiometric normalization methods: Overview and an application to landsat images. *Journal of Geodesy and Cadastre, RevCAD*, 17, 193–200.
- Wright, N., Duncan, J. M. A., Callow, J. N., Thompson, S. E., & George, R. J. (2025). Training sensor-agnostic deep learning models for remote sensing: Achieving state-of-the-art cloud and cloud shadow identification with OmniCloudMask. *Remote Sensing of Environment*, 322, 114694. <https://doi.org/10.1016/j.rse.2025.114694>
- Yu, L., Zhang, Y., Sun, M., Zhou, X., & Liu, C. (2017). An auto-adapting global-to-local color balancing method for optical imagery mosaic. *ISPRS Journal of Photogrammetry and Remote Sensing*, 132, 1–19. <https://doi.org/10.1016/j.isprsjprs.2017.08.002>
- Yuan, X., Cai, Y., & Yuan, W. (2023). Voronoi centerline-based seamline network generation method. *Remote Sensing*, 15(4). <https://doi.org/10.3390/rs15040917>